# Design and System Demonstration of a Tunable Slow-Light Delay Line Based on Fiber Parametric Process

Lilin Yi, *Student Member, IEEE*, Weisheng Hu, *Member, IEEE*, Yikai Su, *Member, IEEE*, Mingyi Gao, and Lufeng Leng, *Member, IEEE*

***Abstract*—We design a tunable slow-light delay line based on fiber-optic parametric process by shaping the gain bandwidth, with its operating wavelength in the present telecommunication window. We derive an analytical expression for the time delay and perform simulations for the delay lines made of dispersion-shifted fiber (DSF) and nonzero dispersion-shifted fiber, respectively. We also experimentally demonstrate the system performance of slow light by propagating 10-Gb/s return-to-zero data packets through such a tunable delay line based on DSF.**

***Index Terms*—Delay line, dispersion, nonlinear, parametric process, slow light.**

## I. Introduction

SLOW LIGHT, referring to manipulating dispersion to slow down the group velocity of pulses of light, is a promising technology for packet synchronization in future all-optical communication networks. Electromagnetic induced transparency (EIT) in an atomic vapor [1] and coherent population oscillation (CPO) in a solid-state crystal [2] are two approaches to optical control of the group velocity of light pulses. Recently, slow light in fibers [3]–[6] are rapidly developing for their compatibility with fiber-optic communication systems. Several slow-light schemes have been demonstrated based on stimulated Brillouin scattering (SBS) [3], [4], stimulated Raman scattering (SRS) [5], and Raman-assisted parametric amplification (FOPA) [6] in fibers. Among them, the bandwidth of the SBS-based scheme is limited to about 12 GHz due to anti-Stokes absorption [4]. The SRS slow light can delay femtosecond pulses, but the delay time is only 370 fs [5]. The Raman-assisted FOPA scheme offers a compromise, and has achieved delay of several bits at a bit rate of tens of gigabits per second [6]. However, to obtain the Raman-assisted effect, the signal wavelength had to be $\sim$100 nm away from the pump wavelength and was therefore out of the 1.55-$\mu$m telecommunication window. Furthermore, none of the previous slow-light schemes has been evaluated in terms of system performance by measuring the bit-error rate (BER) of delayed optical data.

Manuscript received June 30, 2006; revised October 9, 2006. The work of L. Leng was supported by PSC-CUNY under Grant PSCREG-37-435.

L. Yi, W. Hu, Y. Su, and M. Gao are with the State Key Lab of Advanced Optical Communication Systems and Networks, Shanghai Jiao Tong University, Shanghai 200240, China (e-mail: yikaisu@sjtu.edu.cn).

L. Leng is with the New York City College of Technology, City University of New York, New York, NY 11201 USA.

Color versions of Figs. 1 and 3–5 are available at http://ieeexplore.ieee.org.

Digital Object Identifier 10.1109/LPT.2006.887192

Recently, for the first time, we demonstrated the system performance of a FOPA-based slow-light delay line operating in the telecommunication waveband [7]. In this work, we further studied the slow-light delay line by theoretical analysis, simulations, and experiments. We theoretically derived the expression of the time delay based on the parametric amplification without Raman assistance and analyzed the impact of the fiber parameters, the pump, and the signal on the time delay. Simulations show that the nonzero dispersion-shifted fiber (NZDSF) is suitable for delaying shorter wavelength signals, while the DSF with proper zero-dispersion wavelength is more effective in delaying longer wavelength signals in the conventional telecommunication window (1525–1610 nm). Moreover, we experimentally demonstrated the system performance of 10-Gb/s return-to-zero (RZ) data packets delayed by a FOPA based on an available DSF. We investigated the pulse distortion effects and the corresponding BER penalties, which mainly result from the parametric-gain saturation, to understand the limitation of the method. Our experiment verifies the feasibility of fine-tuning the time delay of 10-Gb/s packets, and indicates that higher speed data can be supported by the FOPA-based slow-light delay line.

## II. Theory and Simulation

When a signal falls near an optical resonance, both the real and imaginary parts of the refractive index vary with the optical frequency. The imaginary part of the refractive index represents gain or absorption, while the variation in the real part leads to phase shift. The imaginary and real parts are Hilbert transform pairs [5]. The phase variation with the optical frequency results in the change of the group velocity and the subsequent time delay.

The nonlinear phase variation in the signal lightwave through the parametric process can be expressed as [6]

$$\begin{aligned}\Delta \mathrm{B} &= \mathrm{Im}\left(i\gamma P_0 E_3^*/E_2 \exp\left[i(2\gamma P_0 - \Delta\beta)z\right]\right) \\ &= -(\gamma P_0 + \Delta\beta/2)(G_s - 1)/G_s \end{aligned} \quad (1)$$

where $\gamma$ is the nonlinear coefficient, $P_0$ is the pump power, and $G_s$ is the signal gain. $G_s$ is proportional to the fiber length and the pump power, and inversely proportional to the detuning between the pump and signal wavelengths. $E_2$ and $E_3^*$ indicate the amplitude of the pump and the conjugate amplitude of the signal, respectively, $\Delta\beta = \beta^{(2)}\Omega^2 + 1/12\beta^{(4)}\Omega^4$ is the wave-vector mismatch. Here, $\beta^{(2)}$ and $\beta^{(4)}$ are respectively the second- and fourth-order derivatives of the propagation constant, and $\Omega = \omega_s - \omega_p$ is the frequency detuning between the signal and the pump.

1041-1135/$20.00 © 2006 IEEE

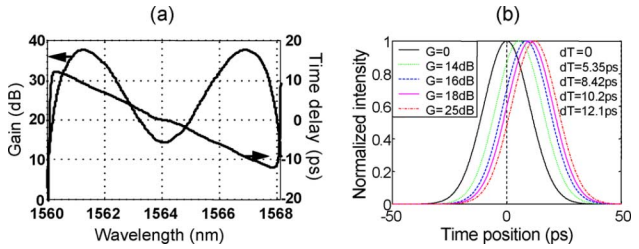


Fig. 1. (a) FOPA gain spectrum and the corresponding time delay. (b) Pulse positions for different signal gains at the signal wavelength of 1560.34 nm.

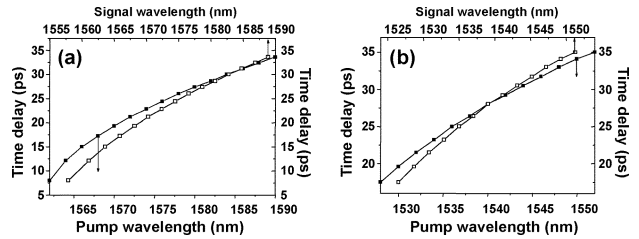


Fig. 2. Maximum time delays versus the pump and signal wavelengths (a) parameters: 5-km DSF, dispersion slope 0.08 ps/(nm$^2$km), zero-dispersion wavelength 1560 nm, pump power 0.56 W. (b) Parameters: 5-km large area NZDSF, dispersion slope 0.12 ps/(nm$^2$km), zero-dispersion wavelength 1520 nm, pump power 0.56 W.

The time delay of the pulses induced by the additional phase shift is described as

$$\Delta T = \int_0^L \frac{\partial \Delta B(z,\omega)}{\partial \omega} dz = \int_0^L \left( -\frac{1}{2}\left(1-\frac{1}{G_s}\right)\frac{\partial \Delta\beta}{\partial \omega} - \frac{(\gamma P_0 + \Delta\beta/2)}{G_s^2}\frac{\partial G_s}{\partial \omega} \right) dz \quad (2)$$

where

$$\partial \Delta\beta/\partial\omega = 2\beta^{(2)}(\omega-\omega_p) + 1/3\beta^{(4)}(\omega-\omega_p)^3 \quad (3)$$

and

$$\partial G_s/\partial\omega = \left((\gamma P_0)^2(\gamma P_0 + \Delta\beta/2)\sinh(gz) \cdot (\sinh(gz) - gz\cosh(gz))/g^4\right) \cdot (\partial\Delta\beta/\partial\omega) \quad (4)$$

where $g^2 = (\gamma P_0)^2 - (\gamma P_0 + \Delta\beta/2)^2$.

Equation (2) indicates that the time delay depends on the signal gain, the fiber dispersion coefficient, the fiber nonlinear coefficient, and the pump power. Based on the above equations, simulations were performed to investigate the time delay induced by a FOPA. The 5-km DSF in the numerical model has these characteristics: dispersion slope 0.08 ps/(nm$^2$km), zero-dispersion wavelength 1560 nm, and effective mode area 54.76 $\mu$m$^2$. The pump wavelength is 1564.1 nm and the power is 0.56 W.

In Fig. 1(a), it is clearly seen that the maximum time delay of 12.1 ps occurs at the signal wavelength of 1560.34 nm. For the signal wavelength of 1567.88 nm, the time delay is $-12.1$ ps, corresponding to fast light. Steeper slope of the gain curve leads to larger time delay. Therefore, the time delay depends on the spectral characteristics of the signal gain. Furthermore, the signal gain varies with the pump power, which induces different time delays of the signal pulse, as shown in Fig. 1(b). We fixed the pump and signal wavelengths at 1564.1 and 1560.34 nm, respectively, and tuned the pump power.

The wavelength separation between the pump and the zero-dispersion wavelength of a fiber has a significant impact on the signal gain bandwidth, and thus affects the time delay. The gain bandwidth becomes narrower with increasing the wavelength separation, which leads to larger time delay, as shown in Fig. 2(a). When the pump wavelength is 1590 nm, the 3-dB gain bandwidth is 0.45 nm, and the maximal time delay at 1588.9 nm is 33.6 ps. For a FOPA, lower dispersion slope leads to a broader gain bandwidth based on the phase-matching condition. However, for a FOPA-based slow-light delay line, a narrow gain bandwidth is required, so the fiber with a high dispersion slope is preferred. Usually, large area NZDSF has a higher dispersion slope than DSF does. The variation of the time delay with the pump and signal wavelengths in a NZDSF is shown in Fig. 2(b). The NZDSF has an effective mode area of 72 $\mu$m$^2$, and a dispersion slope of 0.12 ps/nm$^2$km at the zero dispersion wavelength of $\sim$1520 nm [8]. Due to the larger effective mode area, the nonlinear coefficient of the fiber is smaller, which leads to less signal gain for the same amount of pump power; however, the higher dispersion slope also plays a role and maintains the large time delay. Such a NZDSF-based slow-light delay line can delay shorter wavelength signals in the telecommunication window. In Fig. 2(b), when the pump wavelength is 1552 nm, the 3-dB gain bandwidth is 0.3 nm, and the maximal time delay at 1551.27 nm is 35 ps.

## III. Experiment

Based on the preceding analysis and simulations, an experiment was performed to demonstrate the time delay induced by the parametric process. In this experiment, a DSF was used for its availability. The experimental setup is shown in Fig. 3. Two tunable laser sources (TLSs) serve as the parametric pump and the signal source, respectively. The pump is sent to an intensity modulator (IM) driven by an electrical pulse source with 1.28-ns pulse width and 10% duty cycle. The modulated pump is preamplified by an erbium-doped fiber amplifier (EDFA) and subsequently boosted by a second high-power EDFA. A tunable filter (TF) is inserted after EDFA2 for removing the strong amplification spontaneous emission (ASE). The signal is intensity-modulated by a 10-GHz clock and a 10-Gb/s NRZ data pattern to generate a 10-Gb/s RZ data packet. The data packet is a fixed pattern "10111" followed by 123 "0"-bits and all the "1" bits fall within the pump pulse duration through synchronization between the pump and signal pulses. The insets in Fig. 3 are the waveforms of the pump and the signal, respectively. They are combined by a 95/5 coupler and then sent into a spool of 5-km DSF, whose parameters are the same as those used in the simulations. The signal is then separated from the pump power by TF2 after being amplified and delayed in the DSF. A variable optical attenuator (VOA) is used to control the amplified signal power. Finally, the signal is split four ways and simultaneously measured/monitored by a power meter (PM), an optical spectrum analyzer (OSA), an oscilloscope, and a bit-error-rate tester (BERT).

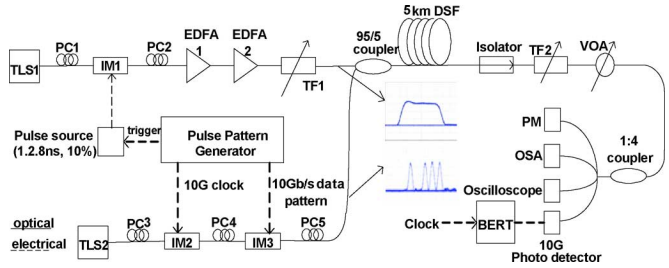


Fig. 3. Experimental setup.

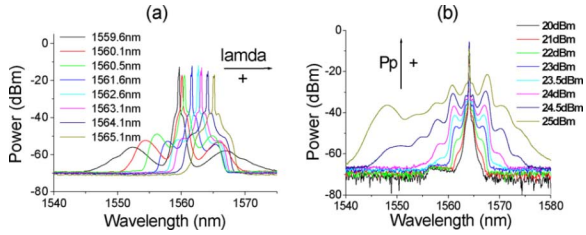


Fig. 4. Measured ASE spectra with 0.2-nm resolution. (a) ASE spectra at 22-dBm average pump power and variable pump wavelengths. (b) ASE spectra at 1564.1-nm pump wavelength and variable pump powers.

To achieve considerable time delay, high gain and narrow gain bandwidth in the FOPA are necessary. In the experiment we measured the ASE spectrum to indicate the signal gain spectrum of the FOPA, as there is a linear relationship between the ASE and the gain for a lossless FOPA. First, we measured the ASE spectra employing a fixed average pump power of 22 dBm at different pump wavelengths, as depicted in Fig. 4(a). When the pump wavelength is larger than the zero-dispersion wavelength of the DSF, the parametric process produces two gain peaks on each side of the pump wavelength. As the pump wavelength increases, the two gain peaks become narrower and closer to the pump wavelength, and the peak gain becomes higher. Signals falling into the shorter wavelength gain peaks experience the time delay. We choose 1564.1 nm as the pump wavelength because of the relatively narrow signal gain spectrum and the shorter wavelength gain peak being close to ITU-T CH 40 (1561.419 nm). In the following experiments, the signal wavelength was set at 1561.4 nm. We then measured the ASE spectra at different pump powers, shown in Fig. 4(b), to study the impact of the pump power on the gain spectra. Once the pump power exceeds 23 dBm, the gain bandwidth is rapidly broadened because of the strong nonlinearity resulting from the high pump power. To achieve good delay performance, it is necessary to balance between the peak gain and the gain bandwidth.

We then investigated the impact of the pump power on the delay time, the waveforms, and the BER of the signal at 1561.4 nm, respectively, as shown in Fig. 5. When the pump power is 21 dBm, corresponding to a 20-dB gain, the delay of the pulse is 10 ps. No pulse distortion is observed, and BER measurement indicates a 0.3-dB sensitivity penalty. When the pump power is increased to 23 dBm and the corresponding gain goes to 37 dB, the delay is enhanced to 15 ps, and the sensitivity penalty is 0.6 dB. Meanwhile, no noticeable distortion of the signal pulses is observed. However, once the pump power exceeds 23 dBm, the gain bandwidth is significantly broadened as shown in Fig. 4(b), resulting in a shorter delay time even though the gain is a little bit enhanced. A 24-dBm pump power leads to a 12-ps delay; however the pulses are broadened and

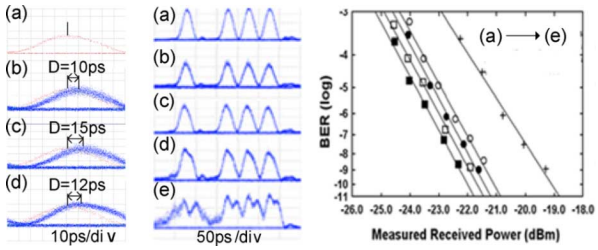


Fig. 5. Delay time, waveform, and BER of the signal versus the pump power. (a) $P = 0$, $G = 0$. (b) $P = 21$ dBm, $G = 20$ dBm. (c) $P = 23$ dBm, $G = 37$ dBm. (d) $P = 24$ dBm, $G = 40$ dBm. (e) $P = 24.5$ dBm, $G = 40$ dBm.

distorted because of the parametric-gain saturation. If the pump power is further increased, the signal pulses are drastically distorted, and the sensitivity penalty is as high as 3 dB.

In this experiment, the maximal delay of the signal at 1561.4 nm is limited to $\sim$15 ps due to a tradeoff between the desired high gain and narrow gain bandwidth. Larger delays of the longer wavelength signals could be achieved by increasing the pump wavelength, as shown in the simulation, but the close spacing between the gain peak and the pump wavelength would make it difficult to separate the pump from the signal.

In this demonstration, tunable time delay is achieved for 10-Gb/s RZ data packets in a FOPA-based slow-light delay line, which could be applied to traffic synchronization. Higher speed data would be delayed in such a delay line, as the gain bandwidth is broad enough and the parametric process is transparent to data rates.

## IV. Conclusion

We have theoretically analyzed and numerically simulated a tunable slow-light delay line based on fiber parametric process in the 1.55-$\mu$m telecommunication window, and performed system testing of delayed 10-Gb/s RZ data packets in DSF. The measured maximal delay is 15 ps at a pumping level of 23 dBm, and the sensitivity penalty is only 0.6 dB, with no significant pulse distortion observed. The potential for higher bit rates is implied.

## References

[1] L. V. Hau, S. E. Harris, Z. Dutton, and C. H. Behroozi, "Light speed reduction to 17 metres per second in an ultracold atomic gas," *Nature*, vol. 397, pp. 594–598, Feb. 1999.

[2] M. S. Begilow, N. N. Lepeshkin, and R. W. Boyd, "Superluminal and slow-light propagation in a room temperature solid," *Science*, vol. 301, no. 5630, pp. 200–202, Jul. 2003.

[3] K. Y. Song, M. G. Herraez, and L. Thevenaz, "Observation of pulse delaying and advancement in optical fibers using stimulated Brillouin scattering," *Opt. Express*, vol. 13, no. 1, pp. 82–88, Jan. 2005.

[4] Z. Zhu, A. M. C. Dawes, D. J. Gauthier, L. Zhang, and A. E. Willner, "12-GHz bandwidth SBS slow light in optical fibers," presented at the Proc. OFC, 2006, Paper PDP1.

[5] J. E. Sharping, Y. Okawachi, and A. L. Gaeta, "Wide bandwidth slow light using a Raman fiber amplifier," *Opt. Express*, vol. 12, no. 16, pp. 6092–6098, Aug. 2005.

[6] D. Dahan and G. Eisenstein, "Tunable all optical delay via slow and fast light propagation in a Raman assisted fiber optical parametric amplifier: A route to all optical buffering," *Opt. Express*, vol. 13, no. 16, pp. 6234–6249, Aug. 2005.

[7] L. Yi, W. Hu, Y. Su, L. Leng, J. Wu, X. Tian, G. Zhou, and L. Zhan, "Propagation of 10-Gb/s RZ data through a slow-light fiber delay-line based on parametric process," presented at the Proc. OFC, 2006, Paper OFH3.

[8] A. Woodfin, J. Painter, and B. Ruffin, Advances in optical fiber technology for analog transport-technical advantages and recent deployment experience [Online]. Available: http://www.corning.com/docs/opticalfiber/NCTA_2003.pdf